confirms that the resonances 1 and 10 have reasonably equal intensities. Starting, on the other hand, from the fact that the pair of rotamers I_6/I_8 has the highest population among those with only two resonances as shown by the inequalities of (3), we assign the resonances 4α and 13β to this pair. An argumentation, similar to that above, leads to an assignment of signals 3α and 5α and 12β and 14β to the pair of rotamers I_5/I_3 and the resonances 7α and 15β to $I_4/I_{\bar{4}}$.

The signal assignment (see Table I) being now achieved, we are able to estimate the experimental rotamer population from the spectrum of Figure 4 of ref 4. To do so, we calculated the surfaces of the triangulated signals of an expansion of this spectrum and computed the population of rotamer r by dividing the sum of the surfaces of the signals associated with rotamer r by the sum of all the signal areas. The populations are given in Table I as x_r^{expll}. We checked then the self-consistency of the rotamer assignment with the choice of M_1 by minimizing the function numerically:

$$F = \sum_{r=1}^{6} (x_r^{\text{expll}} - x_r^{\text{calcd}})^2 \qquad (4)$$

The function F has the minimum value of 2.88×10^{-3} when $z = 0.617$ and $y = 0.539$, which correspond with the values of $G^{\alpha\beta\text{cis}} - G^{\alpha\beta\text{trans}} = 0.22$ kcal/mol and $G^{\beta\beta\text{cis}} - G^{\beta\beta\text{trans}} = 0.29$ kcal/mol at −40 °C, revealing that the $\beta\beta$ interaction is sterically more demanding than the $\alpha\beta$. Using the numerical values of z and y above, we calculated the rotamer populations using eq 2 and the data of Table I. The results, also given in this table, show that the agreement between the experimental rotamer populations and those calculated for M_1 is fairly good.

If we assume, on the other hand, the assignment resulting from mode M_2, i.e., when $I_2/I_{\bar{2}}$ and I_5/I_5 are permuted (see Figures 8 and 9 of ref 4), the minimum value of F is about 8 times larger than the value found for M_1, and the agreement between experimental and calculated populations is poor (see Table I). Moreover, the $\alpha\beta$ interaction appears to be more repulsive ($z = 0.60$; $G^{\alpha\beta\text{cis}} - G^{\alpha\beta\text{trans}} = 0.24$ kcal/mol) than the $\beta\beta$ one ($y = 0.94$; $G^{\beta\beta\text{cis}} - G^{\beta\beta\text{trans}} = 0.03$ kcal/mol). This would in turn mean that the α *o*-tolyl ring is more sterically hindered than the β one, which is very unlikely. We can, therefore, conclude that only the rotamer assignment which was derived with the α one ring rotation M_1 as the threshold mode leads to self-consistent results.

As a consequence of this assignment, the residual β signals at 30° (Figure 3 or ref 4) can now also be attributed more precisely. The one at 1.99 ppm results from the averaging of β signals of I_1, $I_2/I_{\bar{2}}$ and I_3, which have in common that the β methyl groups lie cis to one another. In contrast, the β residual signal at 1.88 ppm is associated with β methyls in trans to one another.

This allows a further assignment of the two signals of 3,4-di-*o*-tolyl-2,5-diphenylcyclopentadienone[10] to the cis rotamer at 2.04 ppm and to the trans rotamer at 1.90 ppm.

In conclusion, this work shows unambiguously that 2D NMR spectroscopy, albeit in conjunction with its 1D counterpart, allows to get a much more precise insight into both the static and dynamic stereochemistry of **1**. The complete rotamer assignment and the more precise evidence for the α one ring rotation as the threshold mode show this undoubtedly.

Experimental Section

The characteristics of compound **1** are given elsewhere.[4] The 2D spectra were recorded at 230 K on a Bruker AM 500 spectrometer, equipped with an aspect 3000 computer and a B-VT 1000 temperature unit. For the exchange experiment a sequence of three pulses, $[90° - t_1 - 90° - \tau_m - 90° - t_2]_n$ was used where τ_m is the so-called mixing time. For this experiment 64 FID'S (of 64 scans each consisting of $512w$ data points) were accumulated, after digital filtering sine bell; the FID was zero-filled to $256w$ in the F_1 dimension. Fourier transformation yielded a spectrum with 1.95 Hz/point digital resolution in both dimensions. Typical acquisition parameters were $sw_1 = \pm 250$ Hz, $sw_2 = 500$ Hz, $\Delta t_1 = 0.2$ ms, 1.5-s recycle delay, and $\tau_m = 80$ ms.

Registry No. 1, 77243-07-3.

^{13}C and ^{1}H EPR Analysis of the Benzo[*a*]pyrene Cation Radical

Paul D. Sullivan,*† Fouad Bannoura,† and Guido H. Daub‡

Contribution from the Departments of Chemistry, Ohio University, Athens, Ohio 45701, and the University of New Mexico, Albuquerque, New Mexico 87131. *Received June 25, 1984*

Abstract: The ^{13}C splittings for benzo[*a*]pyrene (BaP) cation radicals singly labeled at each protonated position have been determined by measuring the increase in the total width of the EPR spectrum of the ^{13}C derivatives over that of the unlabeled parent molecule. The absolute values of the ^{13}C splittings found for the 12 protonated positions (1–12, respectively) are 6.01, 4.55, 4.44, 0.93, 1.32, 8.30, 3.74, 2.91, 3.01, 1.29, 1.96, and 3.60 G. Additionally, with the aid of deuterated BaP and by comparison with computer simulations, an analysis is proposed for the proton splittings in $BaP^{+\cdot}$ in terms of the following 12 splitting constants for positions 1–12, respectively, 4.57, 0.54, 3.77, 0.37, 2.11, 6.63, 2.23, 0.19, 2.95, 1.94, 0.82, and 2.75 G. When the Karplus–Fraenkel theory for ^{13}C splittings is used, the results are compared for internal consistency with those previously estimated from the methylated BaP's. Several deviations from calculated values have been found which may have some significance to the metabolism of BaP and its derivatives.

The electron paramagnetic resonance (EPR) spectrum of the benzo[*a*]pyrene (BaP) cation radical was first observed over 25 years ago[1] and has since been investigated by several groups[2-4] but has so far resisted complete analysis. The analysis of the EPR spectrum is important because of the information it would provide regarding the spin density distribution in the highest occupied molecular orbital (HOMO) of the BaP molecule. Such knowledge would be useful in the correlation of molecular parameters with metabolic products[5,6] as well as regards the speculation that cation

† Ohio University.
‡ University of New Mexico. Deceased June 1984.

(1) Kon, H.; Blois, M. S. *J. Chem. Phys.* **1958**, *28*, 743–744.
(2) Nagata, C.; Inomata, M.; Tagashira, Y. *Gann* **1968**, *59*, 289–298.
(3) Forbes, W. F.; Robinson, J. C.; Wright, G. V. *Can. J. Biochem.* **1967**, *45*, 1087–1098.
(4) Elmore, J. J.; Forman, A. *Cancer Biochem. Biophys.* **1975**, *1*, 115–120.

0002-7863/85/1507-0032$01.50/0

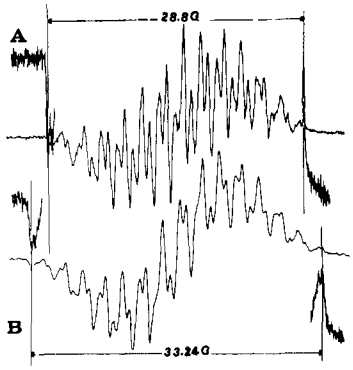

Figure 1. (A) Low-resolution (Mod = 0.8 G) EPR spectra of $BaP^{+\cdot}$ and (B) ^{13}C labeled $BaP^{+\cdot}$ at the 3 position. The insets are the same spectra at higher gain conditions; the measured widths of the unlabeled and labeled BaP's are indicated to be 28.8 and 33.24 G.

radicals of BaP and/or BaP derivatives might have a possible role in the carcinogenic or mutagenic activity of these molecules.[7-9]

The interpretation of the BaP cation radical EPR spectrum is made difficult due to the asymmetry of the molecule which indicates that all 12 protons should be nonequivalent, leading to a maximum possible 2^{12} (4096) lines in the EPR spectrum. Attempts to simplify the spectrum using electron nuclear double resonance (ENDOR) were unsuccessful due to the low signal intensity of the EPR spectrum.[10] In some recent work[11,12] the EPR spectra of the cation radicals of all 12 monomethyl BaP's were investigated, and a method was proposed to estimate and assign the splitting constants for the BaP cation radical. An alternative approach to assigning and estimating the proton splittings in the BaP cation radical has become possible due to the synthesis of BaP's singly labeled with ^{13}C at each of the 12 protonated carbon atoms.[13-16] In this paper the ^{13}C splittings for the BaP cation radical are reported as well as an analysis of the proton splittings. Using the Karplus–Fraenkel theory[17] for ^{13}C splittings the results are compared for internal consistency and the experimental spin densities in the HOMO are contrasted with calculated values.

Materials and Methods

The synthesis of BaP singly labeled at each of the 12 protonated carbon atoms has been previously reported.[13-16] Fully deuterated BaP (99.5%) was obtained from the Merck, Sharp and Dohme Corp. Cation radicals were prepared by dissolving 0.2–0.5 mg of the hydrocarbon in 0.2–0.5 mL of 98% H_2SO_4. After approximately 2 min about 50 μL of the solution was drawn into a capillary tube and placed into the cavity of a Varian E-9 EPR spectrometer. Spectra were recorded at room temperature under various conditions of modulation amplitude and frequency in order to obtain the total width of the spectra and to record high-resolution spectra. Computer simulations of spectra were carried out with previously described programs[18] by using a modified procedure which downloads the simulated data from the IBM 370/158 mainframe to an Apple II+ computer which then plots the spectrum on a chart recorder.

Table I. Carbon-13 Splitting Constants of BaP Cation Radical

position	splitting constant, G	calcd splittings A[a]	calcd splittings B[b]
1	6.01	6.07	5.92
2	4.55	−4.83	−4.83
3	4.44	5.07	4.57
4	0.93	−0.56	−1.11
5	1.32	2.47	1.45
6	8.30	8.43	8.43
7	3.74	2.92	3.93
8	2.91	−2.79	−2.79
9	3.01	2.87	2.73
10	1.29	1.01	1.29
11	1.96	−2.39	−1.97
12	3.60	3.86	3.71

[a] Calculated from spin densities derived from proton splittings (Table II). [b] Improved calculation using estimates for spin densities at blind positions.

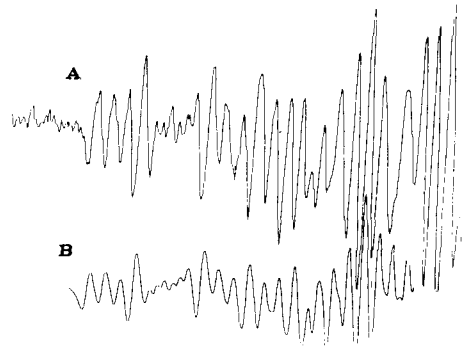

Figure 2. (A) Expanded high-resolution EPR spectrum (Mod = 0.08 G) of the BaP cation radical in H_2SO_4; only the low field end of the spectrum is shown. (B) Simulation of the EPR spectrum using nine proton splittings of 0.188, 0.372, 0.541, 0.824, 1.940, 2.110, 2.230, 2.750, and 2.95 G.

Results and Discussion

The ^{13}C splitting constants can be obtained by simply measuring the increase in the total width of the EPR spectrum of the ^{13}C derivative over that of the protonated derivative. Figure 1 indicates that under low-resolution conditions, it is relatively easy to unambiguously locate the outermost lines of the spectra and hence to measure the total width. In practice the wings of the spectra of the ^{13}C derivative were measured in a dual-sample cavity relative to a perylene cation radical secondary standard, in order to more accurately measure the total width of the spectrum. The values for the ^{13}C splitting constants (Table I) depend upon the spin densities on adjacent carbon atoms (j) as well as the spin density on the central carbon (i) according to eq 1 (for a $CC_2'H$ fragment).[17] When the experimental ^{13}C splittings are used, it is,

$$a_i^C = 35.6\rho_i - 13.9\sum_j \rho_j \qquad (1)$$

therefore, possible to calculate some, but not all, of the spin densities in the BaP molecule and hence estimate some of the proton splittings. However, an alternative procedure which has been adopted is to attempt an analysis of the proton spectra and then use the spin densities obtained from this analysis to calculate the ^{13}C splittings.

In order to analyze the proton splittings, the wing lines of a high-resolution spectrum of BaP in H_2SO_4 were carefully recorded to obtain the best possible signal consistent with a reasonable signal-to-noise ratio (see Figure 2). Then, by painstakingly adding one splitting constant after another, a simulation of the wings was slowly built up. The smallest five splittings (0.19, 0.37, 0.54, 0.825, and 1.94 G) were relatively easily obtained and are unambiguous. The next four splittings (2.11, 2.23, 2.75, and 2.95 G) were more

(5) Loew, G. H.; Wong, J.; Phillips, J.; Hjelmeland, L.; Pack, G. *Cancer Biochem. Biophys.* **1978**, *2*, 123–130.
(6) Fu, P. P.; Harvey, R. G.; Beland, F. A. *Tetrahedron* **1978**, *34*, 857–866.
(7) Wilk, M.; Bez, W.; Rochlitz, J. *Tetrahedron* **1966**, *22*, 2599–2608.
(8) Fried, J. In "Chemical Carcinogenesis Part A"; Ts'o, P. O. P., DiPaolo, J., Ed.; Marcel Dekker: New York, 1974; pp 197–215.
(9) Cavalieri, E.; Rogan, R.; Roth, R. In "Free Radicals and Cancer"; Floyd, R. A., Ed.; Marcel Dekker: New York, 1982; pp 117–153.
(10) Experiments conducted in colllaboration with Dr. R. C. Sealey, National Biomedical ESR Center, Medical College of Wisconsin.
(11) Sullivan, P. D. *J. Magn. Reson.* **1983**, *54*, 314–318.
(12) Sullivan, P. D.; Bannoura, F.; Roach, S. In "Polynuclear Aromatic Hydrocarbons: Mechanisms, Methods and Metabolism"; Dennis, A. J., Cooke, M., Eds.; Battelle Press: Columbus, OH, in press.
(13) Bodine, R. S.; Hylarides, M. D.; Daub, G. H.; VanderJagt, D. L. *J. Org. Chem.* **1978**, *43*, 4025–4028.
(14) Simpson, J. E.; Daub, G. H.; VanderJagt, D. L. *J. Labeled Compd. Radiopharm.* **1980**, *17*, 895–900.
(15) Daub, G. H. *Prepr. Div. Pap.—Am. Chem. Soc., Fuel Chem.* **1980**, *25*, 503.
(16) Unkefer, C. J.; London, R. E.; Whaley, J. W.; Daub, G. H. *J. Am. Chem. Soc.* **1983**, *105*, 733–735.
(17) Karplus, M.; Fraenkel, G. K. *J. Chem. Phys.* **1961**, *35*, 1312–1323.
(18) Forbes, W. F.; Sullivan, P. D.; Wang, H. *J. Am. Chem. Soc.* **1967**, *89*, 2705–2711.

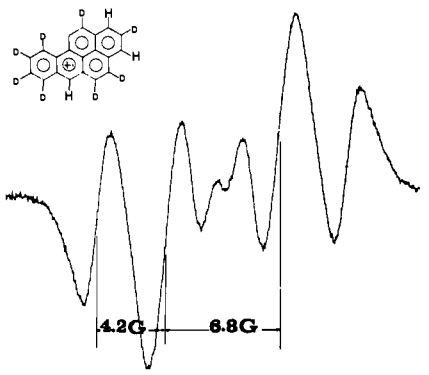

Figure 3. EPR spectra of fully deuterated BaP in H_2SO_4; splittings are a 4.2-G triplet and 6.80-G doublet.

Table II. Proton Splittings of BaP Cation Radical

proton splittings for $BaP^{+\cdot}$, G	position assignment on basis of methyl BaP's	alternative position assignments	spin densities $a/28$
0.188	8	8	(−)0.0067
0.372	4	4	(+)0.0133
0.541	2	2	(−)0.0193
0.824	11	11	(−)0.0294
1.94	10	10	0.0693
2.11	5	5	0.0743
2.23	7	7	0.0793
2.75	1	12	0.0971
2.95	12	9	0.105
3.77	9	3	0.135
4.57	3	1	0.163
6.63	6	6	0.237

difficult to find, and their analysis is known with somewhat less certainty. The simulation of the wing lines using these nine splittings is, however, in reasonable agreement with the experimental spectrum (Figure 2). Having simulated literally hundreds of combinations, we are reasonably confident that these splitting constants are correct within ±0.03 G. In order to find the three largest proton splitting constants, a fully deuterated BaP sample was dissolved in H_2SO_4. It is known[19] that the protons at the 1, 3, and 6 positions of BaP are readily exchangeable in D_2SO_4; thus, the deuteriums at positions 1, 3, and 6 should be exchanged for protons in H_2SO_4. The spectrum which is obtained (Figure 3) consists of a doublet of triplets, thus indicating that the largest splitting is approximately 6.80 G and the average of the next two largest splittings is ca. 4.20 G. Going back to the high-resolution protonated spectra splittings of 3.77, 4.57 G and 6.63 G were obtained. This completed the analysis of the proton spectrum in terms of 12 splittings whose sum corresponds to 28.8 G, equal to the measured total width of the spectrum.

The next major problem is to assign the splittings to specific positions in the molecule. One method of assigning the splittings is by comparison with the monomethylated BaP cation radicals.[11,12] Using the values for the methyl splitting constants, one can assign the proton splittings in order of their absolute values. This leads to the assignments shown in Table II. A major problem with these assignments concerns the magnitude of the proton splitting at the 1 position, which according to the methyl splittings should be the fifth largest splitting. However, as is seen from the deuterated BaP, the average of the 1 and 3 splittings should be 4.2 G; additionally the ^{13}C splitting of the 1 position (6.01 G) is greater than that of the 3 position (4.44 G). The two latter observations are more consistent with an alternate assignment in which the 1 position is assigned as the second largest splitting constant. All the other splittings remain in the same order (see Table II). Possible reasons for an incorrect assignment based on the methyl splittings is the implicit assumption that methyl substitution does not greatly change the spin density distribution; this may not be the case for all positions. Further evaluation of this point must await the complete analysis of the spectra of the monomethylated derivatives.

Using the alternate set of assignments, one can now calculate the spin densities at the protonated positions assuming McConnell's relationship $\rho_i = a_{CH}^H/28$. In previous work with the anthracene cation and anion radicals, Bolton and Fraenkel[20] found that a Q_{CH}^H value of 27 G gave the most consistent agreement between spin densities calculated from the proton splittings and the ^{13}C splittings calculated from the Karplus–Fraenkel equation. In the case of benzo[*a*]pyrene slightly better agreement is found if a Q_{CH}^H value of 28 G is used. When the spin densities calculated from the proton splittings are used, the ^{13}C splittings at the protonated positions can be calculated (see Table I). Unfortunately, since the ^{13}C splitting depends on spin densities at adjacent carbons, one can only do a complete calculation for positions 2, 8, and 9. Even then complications arise for these positions since the small proton splittings at positions 2 and 8 may correspond to positive or negative spin densities. Assuming positive spin densities the ^{13}C splittings are calculated to be −3.45, −2.32, and 2.68 G, respectively. For negative spin densities at the 2 and 8 positions, one calculates ^{13}C splittings of −4.83, −2.79, and 2.87 G. The latter values are clearly in better agreement with the experimental absolute values of 4.55, 2.91, and 3.01 G. For the other positions the ^{13}C splittings were calculated assuming that spin densities at the blind positions are zero (see column A in Table I). Two further assumptions were required, in that the better fit was obtained if the spin density at the 4 position is positive while that at the 11 position is negative. The spin densities at all other positions are taken to be positive. Clearly the overall agreement with the absolute experimental values is quite good except perhaps for the 5 and 7 positions. Even better agreement can be obtained if the spin densities at the blind positions are appropriately adjusted. Since the spin densities at these positions only effect the ^{13}C splittings at adjacent positions they can be individually adjusted to minimize the square of the deviations of the ^{13}C splittings. Thus, a value of $\rho_{13} = 0.011$ minimizes the deviations of the ^{13}C splittings at positions 1 and 12, similarly $\rho_{14} = 0.0352$ minimizes the deviations at positions 3 and 4. In the same manner $\rho_{15} = 0.073$, $\rho_{16} = -0.073$, $\rho_{17} = -0.0201$, and $\rho_{18} = -0.0309$ were obtained and the splittings in column B of Table I were calculated using these additional spin densities. The effect of these adjustments is to reduce the sum of the squares of the deviations between the experimental and calculated ^{13}C values from 3.50 in column A to 0.229 in column B of Table I.

The agreement between the calculated ^{13}C splittings based on the spin densities derived from the proton splittings is sufficiently consistent to provide further justification of the proton assignments. Although small changes in the assignments could be made (i.e., exchange 9 and 12 or 10 and 5, change the order to $11 < 2 < 8 < 4$) which would decrease the sum of the squares of the deviations by small amounts, these changes cannot be justified without knowledge of the spin densities at the blind positions. The spin densities listed in Table II can, therefore, be expected to provide a reasonable picture of the HOMO of BaP. The values are certainly known in sufficient detail that they can be used to test various calculational models as well as to rationalize the chemistry and biology of BaP.

Table III shows the results of a McLachlan[21] modified Hückel molecular orbital calculation of the spin densities and proton splittings as compared to the assigned values. Considering the approximate nature of the calculation, the overall agreement with the general features of the experimental values is quite good. Thus, the calculation reproduces the order and magnitude of the largest splittings, $6 > 1 > 3$, and indicates that the 2, 8, and 11 positions have the smallest splittings. However, the calculation appears to underestimate the spin density at the 9 and 10 positions while

(19) Cavalieri, E.; Calvin, M. *J. Chem. Soc., Perkin Trans. 1* **1972**, 1253–1256.

(20) Bolton, J. R.; Fraenkel, G. K. *J. Chem. Phys.* **1964**, *40*, 3307–3320.
(21) McLachlan, A. D. *Mol. Phys.* **1960**, *3*, 233–252.

Table III. Calculated and Experimental Spin Densities and Proton Splittings for the BaP Cation Radical

position	calcd spin density (ρ)	calcd proton splitting[a]	exptl spin density	exptl proton splitting
1	0.1555	4.35	0.163	4.57
2	-0.0403	1.13	(-)0.0193	0.54
3	0.1396	3.92	0.135	3.77
4	0.0890	2.49	0.0133	0.37
5	0.0858	2.40	0.0743	2.11
6	0.2633	7.37	0.237	6.63
7	0.0872	2.44	0.0793	2.23
8	-0.0172	0.48	(-)0.0067	0.19
9	0.0583	1.63	0.105	2.95
10	0.0144	0.40	0.0693	1.94
11	0.0143	0.40	(-)0.0294	0.824
12	0.1084	3.03	0.0971	2.75

[a] Calculated from McConnell's equation $|a| = Q|\rho|$, Q = 28 G.

overestimating at the 4 position. Attempts to improve the calculations by allowing the overlap integrals to vary according to the known bond lengths[22] of the BaP molecule did not result in any better agreement. Other more sophisticated calculations of electron densities in the HOMO of BaP, also carried out on idealized geometries, are also in no better agreement with the experimental values.[5,23] Since the spin densities represent one-half of the electron density in the HOMO, and since the latter have been related to the nucleophilic reactivity at the carbon atoms,[5,6] the observed deviations between the calculated and experimental values could have a significant effect on interpretations or rationalizations of metabolic pathways based on calculated values. For example, the high spin density observed at the 9 position could indicate that direct oxygen insertion to form 9-hydroxybenzo[*a*]pyrene may account for part or all of the observed metabolic production of this phenol. Additionally the experimentally observed inequivalence of the 4 and 5 positions which was suggested by our previous studies[11,12] of methylated BaP's is supported by the ^{13}C studies. This inequivalence, which is not reproduced by any method of calculation so far investigated would explain the selective production of 5-hydroxybenzo[*a*]pyrene from the isomerization of benzo[*a*]pyrene 4,5-oxide or from the acid dehydration of benzo[*a*]pyrene-4,5-diol.[24] It is also consistent with the breaking of the C_4–O bond in the enzymatic hydrolysis of benzo[*a*]pyrene 4,5-oxide as observed by Yang et al.[24] However, similar selectivity was not observed by Hylarides et al.[25] in their study of BaP-4,5-oxide.

It is obvious from these results that great care should be exercised when using calculated parameters to explain the biological properties of complex molecules. Experimentally derived quantities such as the HOMO spin densities are important in providing a test for the validity of such calculations, and the values obtained in this work should provide a useful set of data against which more refined calculations can be compared.

Acknowledgment. This work was supported, in part, by Grant CA-34966 awarded by the National Cancer Institute, DHEW, to P.D.S.

Registry No. 1-^{13}C-BaP, 93604-46-7; 2-^{13}C-BaP, 93604-47-8; 3-^{13}C-BaP, 93604-48-9; 4-^{13}C-BaP, 67194-47-2; 5-^{13}C-BaP, 67194-48-3; 6-^{13}C-BaP, 77585-09-2; 7-^{13}C-BaP, 87337-12-0; 8-^{13}C-BaP, 87337-13-1; 9-^{13}C-BaP, 87337-14-2; 10-^{13}C-BaP, 87337-15-3; 11-^{13}C-BaP, 67194-49-4; 12-^{13}C-BaP, 67194-50-7; ^{13}C, 14762-74-4.

(22) Iball, J.; Scrimgeour, S. N.; Young, D. W. *Acta Crystallogr., Sect. B* **1976**, *32*, 328-330.
(23) Shipman, L. L.; In "Carcinogenesis. A comprehensive Survey"; Jones, P. W., Freudenthal, R. I., Eds.; Raven Press: New York, 1978; Vol., 3, pp 139-144.
(24) Yang, S. K.; Roller, P. P.; Gelboin, H. V. *Biochemistry* **1977**, *16*, 3680-3687.
(25) Hylarides, M. D.; Lyle, T. A.; Daub, G. H.; VanderJagt, D. L. *J. Org. Chem.* **1979**, *44*, 4652-4657.

An Advanced Visible-Light-Induced Water Reduction with Dye-Sensitized Semiconductor Powder Catalyst

Takeo Shimidzu,* Tomokazu Iyoda, and Yoshihiro Koide

Contribution from the Division of Molecular Engineering, Graduate School of Engineering, Kyoto University, Sakyo-ku, Kyoto 606, Japan. *Received June 20, 1984*

Abstract: For visible-light-induced water reduction to hydrogen with use of a sacrificial electron donor (triethanolamine), an efficient and durable photocatalyst system with xanthene dye sensitization of particulate platinized semiconductor catalyst is presented. A reductive electron-transfer mechanism from the photoreduced dye to the particulate platinized semiconductor is proposed in the present hydrogen production. The excited triplet state of the dye is a precursor of the reduced dye by the amine, so that the efficiency is determined mainly by the real excited triplet quantum yield of the dye. On the basis of this consideration, a novel use of heavy-atom additives to increase the efficiency of durable xanthene dye sensitized systems is demonstrated.

Significant progress on the photoinduced water reduction to hydrogen has been made independently by two main approaches using a sacrificial electron donor. One is the heterogeneous system, in which a particulate (platinized) semiconductor catalyst (Sc or Sc/Pt) is suspended, with band-gap excitation,[1] and the other is a homogeneous photoinduced redox system containing a sensitizer, an electron relay, and a microdispersed Pt catalyst.[2] However, they have some defects: The former has photoaction with near-UV light and tends to photocorrode with photogenerated positive holes in Sc, and the latter has no anisotropic reaction fields available for charge separation.

(1) Since the Honda-Fujishima effect (Honda, K.; Fujishima, A. *Nature (London)* **1972**, *238*, 37), numerous investigations have been done. So, some reviews are listed herein. (a) Heller, A. *Acc. Chem. Res.* **1981**, *14*, 154. (b) Wrighton, M. S. *Acc. Chem. Res.* **1979**, *12*, 303. (c) Bard, A. J. *J. Photochem.* **1979**, *10*, 59. (d) Memming, R. *Electroanal. Chem.* **1979**, *11*, 1.

(2) Grätzel, M.; Kalyanasundaram, K.; Kiwi, J. "Structure and Bonding. 49. Visible Light Induced Cleavage of Water into Hydrogen and Oxygen in Colloidal and Microheterogeneous System"; Springer-Verlag: New York, 1982.

0002-7863/85/1507-0035$01.50/0